Available online at www.sciencedirect.com

SCIENCE DIRECT

Developmental Biology 278 (2005) 381–395

DEVELOPMENTAL BIOLOGY

www.elsevier.com/locate/ydbio

Notch–Delta signaling is required for spatial patterning and Müller glia differentiation in the zebrafish retina

R.L. Bernardos[a], S.I. Lentz[b], M.S. Wolfe[c], P.A. Raymond[a,d,*]

[a]*Neuroscience Graduate Program, University of Michigan, Ann Arbor, MI, USA*
[b]*Michigan Diabetes Research and Training Center, University of Michigan Medical School, Ann Arbor, MI 48109-0616, USA*
[c]*Center for Neurologic Diseases, Harvard Medical School and Brigham and Woman's Hospital, Boston, MA, USA*
[d]*Department of Cell and Developmental Biology, University of Michigan, Ann Arbor, MI 48109-0616, USA*

Received for publication 27 July 2004, revised 11 November 2004, accepted 12 November 2004
Available online 17 December 2004

Abstract

Notch–Delta signaling has been implicated in several alternative modes of function in the vertebrate retina. To further investigate these functions, we examined retinas from zebrafish embryos in which bidirectional Notch–Delta signaling was inactivated either by the *mind bomb* (*mib*) mutation, which disrupts E3 ubiquitin ligase activity, or by treatment with γ-secretase inhibitors, which prevent intramembrane proteolysis of Notch and Delta. We found that inactivating Notch–Delta signaling did not prevent differentiation of retinal neurons, but it did disrupt spatial patterning in both the apical–basal and planar dimensions of the retinal epithelium. Retinal neurons differentiated, but their laminar arrangement was disrupted. Photoreceptor differentiation was initiated normally, but its progression was slowed. Although confined to the apical retinal surface as in normal retinas, the planar organization of cone photoreceptors was disrupted: cones of the same spectral subtype were clumped rather than regularly spaced. In contrast to neurons, Müller glia failed to differentiate suggesting an instructive role for Notch–Delta signaling in gliogenesis.

Keywords: Notch; Delta; *mind bomb*; Retinal development; Photoreceptors; Müller glia; γ-secretase inhibitors *her*; *Hes*

Introduction

Specification and differentiation of the zebrafish retina is similar to that of other vertebrates although development proceeds very rapidly in this teleost fish. A region in the anterior neural plate becomes determined as the retinal field at the end of gastrulation in zebrafish embryos (8 h post-fertilization; hpf) and is shaped into bilateral optic primordia by 15 hpf (Schmitt and Dowling, 1999; Varga et al., 1999; Woo and Fraser, 1995). Retinal differentiation begins around 23 hpf with the formation of the first retinal ganglion cells (Burrill and Easter, 1994; Hu and Easter, 1999). By 73 hpf, neurogenesis in the central retina is mostly complete, the nuclear and plexiform layers are well differentiated, and visual function begins (Hu and Easter, 1999; Malicki, 1999). The zebrafish retina, as in other vertebrates, contains six primary neuronal cell types (ganglion, amacrine, bipolar and horizontal cells; cone and rod photoreceptors) and one intrinsic glial cell type (Müller glial cells). All retinal neurons and Müller glial cells are derived from a common, multipotent retinal progenitor (Turner and Cepko, 1987).

Notch–Delta signaling has been implicated in several different processes in the developing retina, including maintenance of a proliferating pool of retinal progenitors, lateral inhibitory interactions that prevent differentiation of retinal neurons, and promotion of Müller glial differentiation (Ahmad et al., 2004; Livesey and Cepko, 2001; Mu and Klein, 2004; Perron and Harris, 2000; Pujic and Malicki, 2004). Stage-dependent

* Corresponding author. Department of Cell and Developmental Biology, University of Michigan at Ann Ardor Medical School, 1301 E. Catherine Street, Mail Code 616, Ann Arbor, MI 48109–0616. Fax: +1 734 763 1166.
E-mail address: praymond@umich.edu (P.A. Raymond).

0012-1606/$ - see front matter © 2004 Elsevier Inc. All rights reserved.
doi:10.1016/j.ydbio.2004.11.018

changes in the intrinsic properties of retinal progenitors may account for these different responses to activation of Notch–Delta signaling. Blocking Notch activity early in retinal development with antisense oligonucleotides, or misexpression of Delta, forces progenitors to differentiate prematurely and adopt early neuronal fates, such as retinal ganglion cells (Austin et al., 1995; Dorsky et al., 1997; Silva et al., 2003). The opposite effects have been seen with misexpression of activated Notch, which maintains proliferating, undifferentiated retinal progenitors (Austin et al., 1995; Bao and Cepko, 1997; Rapaport and Dorsky, 1998; Schneider et al., 2001). Gliogenic properties of Notch signaling also have been described in developing retina, in which activated Notch promotes Müller glia differentiation (Bao and Cepko, 1997; Furukawa et al., 2000; Hojo et al., 2000; Scheer et al., 2001). In the zebrafish retina, for example, misexpression of a constitutively active form of Notch in retinal progenitors either promoted the differentiation of Müller glia or the cells remained undifferentiated (Scheer et al., 2001). Similarly, retroviral transduction of activated *Notch1* in the developing rat retina resulted in the expression of glial markers in transfected cells (Furukawa et al., 2000). Additionally, expression of *Hes1*, a basic helix–loop-helix transcriptional repressor gene that acts downstream of Notch to inhibit neurogenesis, has been reported to promote gliogenesis in the retina (Kageyama et al., 1997). In contrast, interfering with *Hes1* function in the rodent retina, either by misexpression of a dominant-negative form of *Hes1* or creation of a *Hes1*-null mutant, results in a decreased number of Müller glia (Furukawa et al., 2000; Takatsuka et al., 2004).

These previous studies of the role of Notch–Delta signaling in retinal development have relied primarily on altering the function of one of the many specific components in the signaling pathways (Ahmad et al., 2004; Livesey and Cepko, 2001; Perron and Harris, 2000; Scheer et al., 2001). Here, we extend the analysis of the role of Notch–Delta signaling in retinal development by using genetic and pharmacological techniques that broadly inhibit both Notch and Delta function in all cells. The zebrafish Notch pathway mutant, *mind bomb* (*mib*), disrupts the catalytic function of a novel RING E3 ubiquitin ligase that is essential not only for signal transduction mediated by Delta but also for efficient Notch signaling in the neighboring cells (Itoh et al., 2003). Bidirectional Notch–Delta signaling is therefore severely compromised in these mutants, and our study examined, for the first time, the consequences on retinal development. We then compared the retinal phenotype in *mib* mutants to the effects of pharmacological disruption of the γ-secretase/presenilin protease complex. This enzyme is important for processing and signal transduction of both Notch and Delta, and inhibiting its activity thereby secondarily blocks transcriptional activation mediated by Notch and Delta (Bland et al., 2003; Ikeuchi and Sisodia, 2003; Kimberly and Wolfe, 2003; LaVoie and Selkoe, 2003; Steiner et al., 1999). We found that neither the *mib* mutation nor inhibition of γ-secretase activity prevented retinal neuron differentiation, although photoreceptor differentiation was slowed, and the planar and laminar organization of all retinal neurons was disrupted. In contrast, in the absence of Notch–Delta signaling, Müller glia failed to differentiate.

Materials and methods

Zebrafish embryos

Wild-type embryos were collected from our outbred zebrafish colony. *Mind bomb* (*mib*^{ta52b}) heterozygous mutant carriers were obtained from John Kuwada. All embryos were raised at 28.5°C and staged according to hours post-fertilization (hpf) and morphological characteristics as described previously (Westerfield, 2000). Some embryos were maintained in 0.03% phenylthiourea (PTU) after 10 hpf to block melanin formation (Westerfield, 2000). All procedures using animals were approved by the Use and Care of Animals in Research Committee at the University of Michigan.

γ-secretase inhibitor treatment

The γ-secretase inhibitor, WPE-III-89, also called Compound E (Seiffert et al., 2000) was used to block bidirectional Notch–Delta signaling by inhibiting intramembrane proteolysis (Kimberly and Wolfe, 2003). Compound E (CE) was prepared as a stock solution (10 mM in 100% DMSO) and then was diluted to a final concentration of 20–100 μM in E2 embryo medium (Nuesslein-Volhard and Dahm, 2002) with 0.03% PTU and 2% DMSO. Embryos at 6–9 hpf (75%–90% epiboly stage) were dechorionated by soaking in 0.1% pronase for 2 min, then rinsed several times in E2 and placed in groups of five to eight embryos per well of a 24-well culture plate. The bottoms of the culture wells were coated with 1.5% agarose to prevent the embryos from sticking to the plastic. Embryos were soaked in either the drug (CE at concentrations up to 100 μM) or a control solution (2% DMSO in E2 media with or without 0.03% PTU) beginning from 6 to 24 hpf. Both drug and control solutions were refreshed every 24 h. Embryos were fixed at 48, 65, 96, or 120 hpf in 4% paraformaldehyde in phosphate buffered saline (PBS) overnight at 4°C.

Immunocytochemistry

Zebrafish embryos were cryoprotected, embedded, and sectioned as described previously (Barthel and Raymond, 1990). Sections were processed for immunocytochemistry as follows: 60 min incubation in blocking reagent (20% normal goat serum, 0.1% sodium azide, PBS, 0.5% Triton X-100); overnight incubation at 4°C with primary antibody diluted in 1% normal goat serum, 0.1% sodium azide, PBS,

0.5% Triton X-100 (diluting reagent); 30 min rinse in washing buffer (1% normal goat serum, 0.1% sodium azide, PBS); 60 min incubation at room temperature with secondary antibody in diluting reagent; 30 min rinse in washing buffer. Slides were coverslipped with anti-fade mounting media (60% glycerol; 0.1 M sodium carbonate; 0.4 mg/ml p-phenylenediamine).

The following monoclonal antibodies that recognize defined structures in zebrafish embryos were obtained from the Zebrafish International Resource Center at the University of Oregon (Eugene, OR): zrf-1 (1:4), which recognizes glial fibrillary acidic protein, GFAP (Marcus and Easter, 1995); zpr-1 (1:400), which labels an unidentified surface epitope on red-green double cones; zn-5 (1:500), which recognizes a surface adhesion molecule of the immunoglobulin superfamily, neurolin/DM-GRASP (Fashena and Westerfield, 1999); zs-4 (1:10), which recognizes an unidentified epitope expressed in the ventricular lining of the nervous system, outer limiting membrane of the retina and the lens epithelium. The Rho4D2 monoclonal antibody (1:100), generated against bovine rhodopsin, was kindly provided by Robert Molday. Antibody to phosphorylated histone H3 (pH3; 1:1000) was from Upstate Biotechnology (Lake Placid, NY). Anti-glutamine synthetase (GS) monoclonal antibody (1:50) was the generous gift of Paul Linser. Anti-islet-1 monoclonal antibody (39.4D5; 1:1000) was from the Developmental Studies Hybridoma Bank (University of Iowa, Iowa City, IA). Anti-calretinin polyclonal antibody (AB5054; 1:1000) was from Chemicon International (Temecula, CA). The following secondary antibodies were used: anti-mouse or anti-rabbit Cy-3 (1:200; Jackson ImmunoResearch Laboratories, Inc., West Grove, PA). The fluorescent DNA-binding dye (4′,6-diamidino-2-phenylindole dihydrochloride, DAPI) was used to stain cell nuclei (Sigma-Aldrich, St. Louis, MO). A 1 mg/ml stock solution of DAPI was diluted 1:500 in PBS. Slides were soaked in the DAPI solution in the dark for 2 min, rinsed for 5 min in PBS and then coverslipped with anti-fade mounting media.

Cell death detection and quantification

TUNEL labeling to reveal nuclear DNA strand breaks generated during cell apoptosis was performed on 6 μm-thick cryosections using an in situ cell death detection kit with alkaline phosphatase converter (Roche Molecular Biochemicals, Indianapolis, IN) per the manufacturer's protocol. Fast Red was used for antibody visualization (Roche Molecular Biochemicals) following the manufacturer's instructions. The level of cell death for each experimental condition ($mib^{-/-}$, mib wild-type sibling, γ-secretase-inhibited and control) was quantified by selecting TUNEL-labeled retinal cryosections with similar maximum lens diameters and co-labeling them with DAPI to mark all cell nuclei present. Total DAPI-labeled nuclei in the neural retina were counted in each section along with TUNEL-labeled cells. The proportion of TUNEL-labeled nuclei to total DAPI-labeled nuclei in control and mutant or γ-secretase-inhibited embryos was compared statistically using a nonparametric, two-tailed Mann–Whitney *U* test.

In situ hybridization

Full length cDNAs encoding zebrafish rod opsin (*rho*) and four cone opsins: red (*opn1lw1*), green1 (*opn1mw1*), blue (*opn1sw2*) and ultraviolet (*opn1sw1*) were kindly provided by David Hyde and Thomas Vihtelic, and *her6* was provided by José Campos-Ortega. Detection of opsin transcripts in whole-mounted eyes by in situ hybridization followed previously published methods (Barthel and Raymond, 1993, 2000) with slight modifications. Typically, two antisense RNA probes were hybridized simultaneously, one labeled with digoxigenin (DIG) and the other labeled with fluorescein (FL) (Roche Molecular Biochemicals). FL-labeled cRNA probes were detected by anti-FL antibodies conjugated with alkaline phosphatase (Roche Molecular Biochemicals) and visualized with Fast Red or 4-nitroblue tetrazolium chloride/5-bromo-4-chloro-3-indolyl phosphate (NBT/BCIP) following the manufacturer's instructions (Roche Molecular Biochemicals). DIG-labeled cRNA probes were detected by anti-DIG antibodies conjugated with peroxidase (Roche Molecular Biochemicals), amplified with a biotinylated-tyramide signal amplification (TSA) kit (Perkin Elmer Life Sciences, Inc., Boston, MA) and visualized with avidin conjugated to fluorescein isothiocyanate (FITC). Individual whole-mount eyes were isolated from the embryos and placed in wells made from a single layer of Parafilm M (American National Can, Greenwich, CT) mounted between a cover glass and microscope slide with anti-fade mounting media. Tissue cryosections were processed similarly for *her6* and opsin detection.

Imaging

Digital images were captured using either an Olympus BX-51 fluorescent microscope or a Zeiss LSM 510 confocal microscope.

Results

Retinal neurons differentiate in mind bomb mutants, but retinal lamination is disrupted

The homozygous mib^{ta52b} embryos exhibited a severe early neurogenic phenotype and other abnormalities characteristic of loss of Notch–Delta signaling, including morphological defects in the hindbrain, trunk somites, and otic vesicle and loss of melanophores in the posterior trunk and tail (data not shown) as originally reported (Haddon et al., 1998; Jiang et al., 1996; Schier et al., 1996). Most homozygous mutant embryos died by 5 days post-fertilization (dpf). We next characterized the retinal

phenotype of the *mib*^{ta52b} mutants, which had not been previously investigated.

The morphology of the retinas from *mib*$^{-/-}$ embryos and wild-type siblings was examined at 65 hpf in cryosections. The retinas of wild-type embryos were laminated by 65 hpf, with a recognizable ganglion cell layer (GCL), inner nuclear layer (INL) and outer nuclear layer (ONL) of photoreceptors, separated by intervening neuropil—the inner (IPL) and outer plexiform layers (OPL) (Fig. 1A). We found that lamination of the inner retina was severely disrupted in *mib*$^{-/-}$ embryos at 65 hpf, and in some retinas irregular clumps of nuclei were clustered around patches of apparent neuropil. In contrast, the morphology of nuclei in the ONL in some regions of *mib*$^{-/-}$ retinas resembled the single row of columnar nuclei characteristic of differentiating photoreceptors in the control retina (Fig. 1B). TUNEL labeling revealed substantial apoptotic cell death in the retina at this stage in *mib*$^{-/-}$ embryos compared to wild-type embryos (Figs. 1C, D; Table 1).

Despite the abnormal laminar organization, especially in the inner retina, several retinal-specific markers indicative of differentiating retinal neurons were found in the *mib*$^{-/-}$ embryos. For example, the retinal ganglion cell-marker, zn-5/neurolin, stained clusters of cell bodies near the inner surface of the retina and their axonal processes, which formed an abnormal optic nerve in the *mib*$^{-/-}$ embryos (Figs. 1E, F). A specific cell-surface marker for red-green double cones, zpr-1, was also expressed in the *mib*$^{-/-}$ retinas, however, the number of double cones was reduced, ranging from 1 to 2 cells to a single row of cells spanning one third of the ONL (Fig. 1H). In contrast, in wild-type embryos at this stage two thirds or more of the linear extent of the ONL contained double cones (Fig. 1G).

To further examine photoreceptor differentiation, we used opsin-specific RNA probes and antibodies. Retinal cryosections from *mib*$^{-/-}$ and wild-type siblings were processed for in situ hybridization with rod opsin RNA probes or for immunocytochemistry with the Rho4D2 rhodopsin antibody. Differentiating photoreceptors expressed rod opsin mRNA (Fig. 1I) or protein (not shown) in wild-type and *mib*$^{-/-}$ retinas at 65 hpf, although opsin-expressing photoreceptors were reduced in the mutants (Fig. 1J). At later stages (73 hpf), rod opsin expression remained restricted to a few cells in the ventral retina of *mib*$^{-/-}$ embryos (data not shown), whereas differentiating rods were distributed across the entire retina of wild-type embryos (Raymond et al., 1995; Schmitt and Dowling, 1996; Stenkamp et al., 1996). The extent of photoreceptor differentiation was assessed

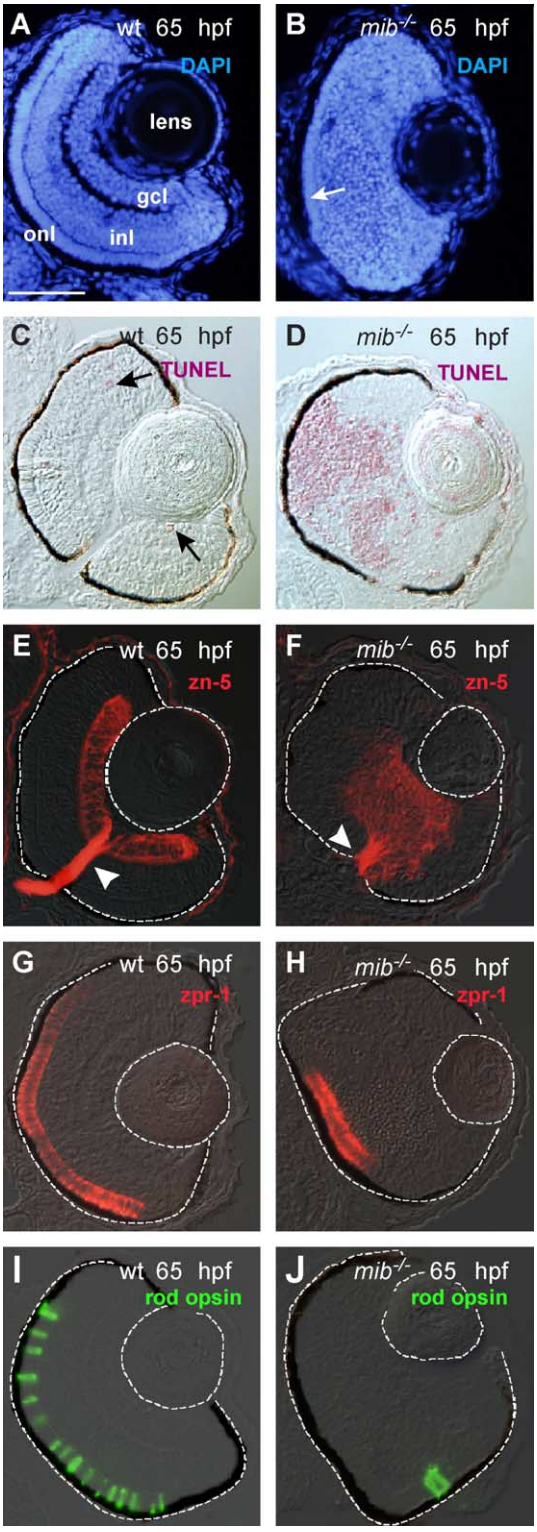

Fig. 1. Differentiation and laminar organization of the retina in wild-type and *mib*$^{-/-}$ embryos at 65 hpf. DAPI-stained wild-type (A) and *mib*$^{-/-}$ (B) retinas. Lamination was absent in the *mib*$^{-/-}$ retina except for an outer nuclear layer (onl; arrow). TUNEL-labeled wild-type (C) and *mib*$^{-/-}$ (D) retinas (Fast Red—red). Representative apoptotic cells are indicated by arrows in the wild-type. Ganglion cells labeled with the zn-5/neurolin antibody in wild-type (E) and *mib*$^{-/-}$ (F) retinas (Cy-3—red; arrowhead = optic nerve; N = 10 embryos examined for each condition). (G–J) Opsin expression in wild-type and *mib*$^{-/-}$ retinas. Expression of red opsin (Cy-3—red) in wild-type (G) and *mib*$^{-/-}$ (H) retinas (N = 10 embryos). Expression of rod opsin (FITC—green) in rod photoreceptors in wild-type (I) and *mib*$^{-/-}$ (J) retinas (N = 10 embryos). Abbreviations: ganglion cell layer (gcl); inner nuclear layer (inl); outer nuclear layer (onl). Dorsal is up and ventral is down in this and all subsequent figures unless otherwise noted. The lens and outer border of the retina in this figure and all subsequent figures has been outlined to orient the reader. Scale bar = 50 μm (A–J).

Table 1
Statistical analysis of TUNEL labeling in *mib*$^{-/-}$, *mib* wild-type sibling (*mib* wt), γ-secretase-inhibited (CE) and control (CNTL) zebrafish retinas

	Number of retinas	Mean no. of TUNEL+ cells	SEM	SD	Compared to *mib*$^{-/-}$	Compared to *mib* wt	Compared to CE	Compared to CNTL
mib$^{-/-}$	13	38.138	2.493	±8.989	N/A	$P = 0.0001$	$P = 0.0018$	$P = 0.0004$
mib wt	10	1.088	0.395	±1.249	$P = 0.0001$	N/A	$P = 0.0001$	$P = 0.474$
CE	7	22.429	0.794	±2.101	$P = 0.0018$	$P = 0.0001$	N/A	$P = 0.0006$
CNTL	7	0.923	0.200	±0.529	$P = 0.0004$	$P = 0.474$	$P = 0.0006$	N/A

Presented above are the means, standard error of the mean (SEM) and standard deviation (SD) for the total number of TUNEL-labeled cells for each experimental condition. The percentage of TUNEL-labeled cells to total number of DAPI-labeled cells present was compared and analyzed using a non-parametric, two-tailed Mann–Whitney *U* test for each experimental condition. *P* values for each comparison are presented above. N/A = not applicable.

further by cataloging the progression of opsin expression across whole-mounted retinas according to a photoreceptor differentiation index, modified from our previous study (Raymond et al., 1995): 1 = no opsin detected in the retina; 2 = opsin expression confined to the ventronasal quadrant; 3 = opsin expression present across two thirds or more of the outer retinal surface. At 65 hpf, the progression of rod opsin expression in *mib*$^{-/-}$ embryos was stalled at an index of 1 or 2 (Fig. 2A; Table 2). These observations suggest that rod photoreceptor differentiation was initiated properly, but did not progress in the mutants.

Cone opsin expression was examined from 56 to 80 hpf, which spans the period of cone differentiation from the initial expression of cone opsin in the ventral patch to complete coverage of the retina by differentiating cones (Raymond et al., 1995; Schmitt and Dowling, 1996). The timing of onset of red cone opsin expression was approximately normal in *mib*$^{-/-}$ embryos, and the earliest differentiating cones in mutant and wild-type embryos were located in the ventral patch, coincident with the first rod photoreceptors as in wild-type embryos (data not shown). By 65 hpf, cone photoreceptors across most of the retina expressed red and UV cone opsin in wild-type embryos (Figs. 2B, C; Table 2), but in *mib*$^{-/-}$ embryos, red and UV opsin expression was significantly reduced (Figs. 2B, C; Table 2). Opsin expression in the *mib*$^{-/-}$ retinas at this stage was discontinuous, and regions that lacked opsin expression appeared to be degenerating (data not shown). By 80 hpf in wild-type embryos, individual photoreceptors expressing either red opsin or green opsin were evenly distributed in a mosaic array across most of the retina, whereas in *mib*$^{-/-}$ embryos red cone photoreceptors had collapsed into irregular clumps separated by regions of degeneration, and green cone opsin expression was typically absent (data not shown).

Retinal gliogenesis is inhibited in mib mutant embryos

Gliogenesis in the *mib*$^{-/-}$ embryos was analyzed using the monoclonal antibody zrf-1 to detect expression of the glial-specific marker, Glial Fibrillary Acidic Protein (GFAP). At 65 hpf, wild-type embryos expressed zrf-1/GFAP in glial cells within the brain and in retinal Müller glia (Fig. 3A). In *mib*$^{-/-}$ embryos, zrf-1/GFAP expression was detectable in the brain, but was absent in the retinas (Fig. 3B). The organization of the glia in the *mib*$^{-/-}$ brains was abnormal compared to wild-type brains (Figs. 3A, B).

To confirm that Notch–Delta signaling was blocked in *mib*$^{-/-}$ embryos, we looked at the expression of a downstream target of Notch signaling, *her6* (an ortholog of *Hes1* in mammals). We found that in the zebrafish retina, *her6/hes1* expression is localized to Müller glia and to progenitors in the germinal zone, and its expression is maintained in these areas in the adult zebrafish (see Supplementary Fig. 1A). This is in contrast to the transient expression of *Hes1* reported in Müller glia in the mouse retina (Hatakeyama and Kageyama, 2004). At 65 hpf, *her6/hes1* was expressed in the ventricular zones of wild-type and *mib*$^{-/-}$ brains (Figs. 3C, D). In the eye, wild-type embryos expressed *her6/hes1* in the retinal germinal zone and lens epithelium, and in the inner nuclear layer

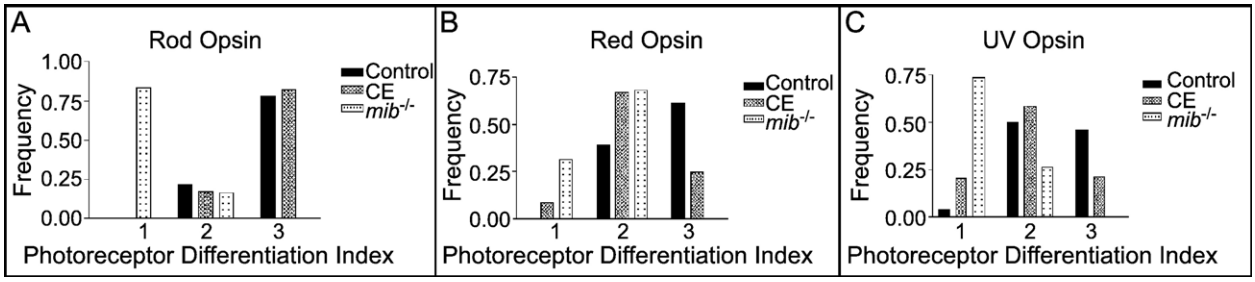

Fig. 2. Frequency histograms of the photoreceptor differentiation index. Levels of photoreceptor differentiation, as measured by opsin expression at 65 hpf in control, *mib*$^{-/-}$ and CE-treated retinas (See text for a description of the index). (A) Rod photoreceptor differentiation progressed normally in CE-treated retinas and controls, but was significantly slowed in *mib*$^{-/-}$ retinas (Table 2). (B) Red cone differentiation was slowed in CE-treated and *mib*$^{-/-}$ retinas compared to controls (Table 2). (C) UV cone differentiation was also slowed in CE-treated and *mib*$^{-/-}$ retinas compared to controls (Table 2).

Table 2
Results of ANOVA pairwise comparisons with Dunn's multiple comparison test, number of eyes examined in each experiment, and number of independent experiments for the data plotted in Figs. 2A, B, C

	CNTL vs. CE	CNTL vs. *mib*$^{-/-}$	*mib*$^{-/-}$ vs. CE	CE and CNTL		*mib*$^{-/-}$ and CNTL	
				Number of eyes examined per experiment	Number of independent experiments	Number of eyes examined per experiment	Number of independent experiments
Rod Opsin	$P > 0.05$	$P < 0.01$*	$P < 0.01$*	8 to 9	2	2 to 7	3
Red Opsin	$P < 0.001$*	$P < 0.001$*	$P < 0.01$*	8 to 36	7	2 to 19	2
UV Opsin	$P < 0.05$*	$P < 0.001$*	$P < 0.001$*	8 to 36	7	2 to 19	2

* P value is <0.05.

(Figs. 3C, C′). In the *mib*$^{-/-}$ retinas, *her6/hes1* expression was absent from the retina and was detectable only in the lens epithelium and brain (Figs. 3D, D′).

γ-secretase-inhibition phenocopies the mind bomb mutation

Treatment of zebrafish embryos with the γ-secretase inhibitor Compound E (CE) at 100 μM beginning at 8 to 9 hpf phenocopied the most obvious phenotypic characteristics of the *mib* mutation that are visible at 2 to 4 dpf, including an abnormal hindbrain, reduced size of eye and ear, and altered somitogenesis, which results in a dorsal flexion of the tail and impaired mobility (Geling et al., 2002). Drug treatment starting later, at 24 hpf, produced embryos with abnormal tail formation but with less obvious hindbrain defects (data not shown). At lower doses, the defects were less severe and not all embryos were affected. The results described below are from experiments in which embryos were treated with 100 μM CE beginning at 8–9 hpf.

We next examined the effects of γ-secretase inhibition on retinal development. In embryos treated with CE beginning at 9 hpf and examined at 65 hpf with the DNA stain, DAPI, the inner retina lacked distinctive nuclear and plexiform layers, but the ONL was typically present, just as in *mib*$^{-/-}$ embryos (Fig. 4B). TUNEL staining revealed increased cell death in the inner retina of γ-secretase-inhibited compared to control embryos at 65 hpf (Figs. 4C, D; Table 1), but apoptosis was not as severe as in the *mib*$^{-/-}$ retinas (compare to Fig. 1D; Table 1). No apoptotic nuclei were found in the photoreceptor layer (ONL) in the γ-secretase-inhibited or control embryos (Figs. 4C, D).

Several markers of retinal differentiation were expressed at 65 hpf in wild-type and γ-secretase-inhibited embryos,

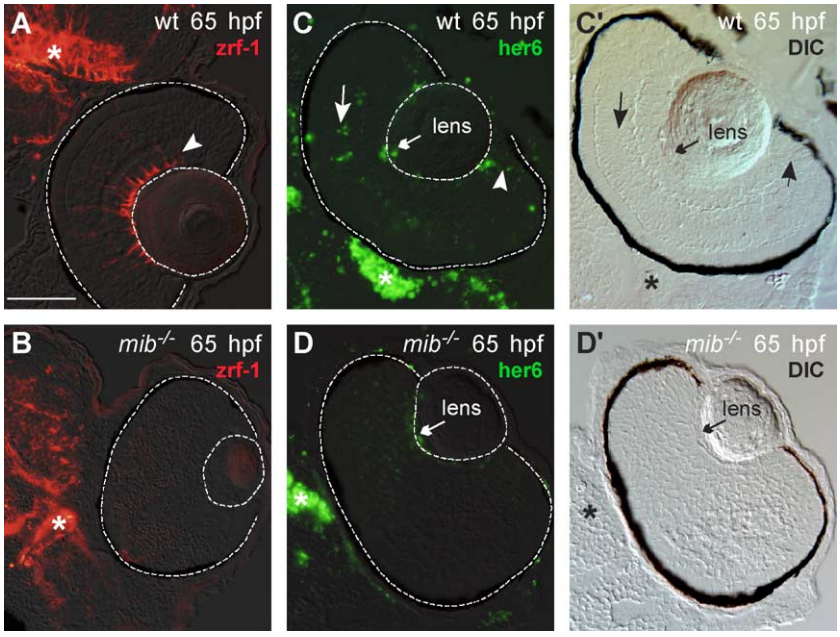

Fig. 3. Müller glia differentiation is inhibited in *mib*$^{-/-}$ retinas at 65 hpf. Müller glia in the retina (outlined) expressed zrf-1/GFAP (arrowhead) as did astrocytes and/or radial glia in the brain (*) of wild-type embryos (A). In contrast, zrf-1/GFAP expression was absent in the retina (outlined) but present in the brain (*) of *mib*$^{-/-}$ embryos (B; $N = 10$). (C, D) Expression of *her6/hes1* in wild-type and *mib*$^{-/-}$ 65 retinas. (C′ , D′) Differential interference contrast (DIC) images of the retinas in (C and D; $N = 8$ embryos). (C, C′) In the wild-type embryos, *her6/hes1* expression was present in the brain (*) and in the germinal zone (arrowhead), lens epithelium (small arrow) and inner nuclear layer (large arrow) of the retina. (D, D′) The *mib*$^{-/-}$ embryos expressed *her6/hes1* in the brain (*) but expression in the eye was restricted to the lens epithelium (small arrow). Scale bar = 50 μm (A–D).

including two markers for retinal ganglion cells, zn-5/neurolin (Figs. 4E, F), and islet-1 (Figs. 4G, H). However, in the γ-secretase-inhibited embryos, the ganglion cell axons followed abnormal trajectories, although many eventually found their way into the optic nerve, despite the disrupted laminar organization of the inner retina (Fig. 4F). Ganglion cells differentiated approximately in their correct location at the inner (basal) surface of the retina, but their cell bodies were not confined to a discrete layer nor were they aligned in an orderly row and instead formed irregular clusters (Fig. 4H). Anti-calretinin, a calcium-binding protein expressed in neurons (Andressen et al., 1993; Schwaller et al., 1993; Yazulla and Studholme, 2001), labeled several classes of cells in the control retinas, including ganglion, amacrine and a subset of bipolar cells (Fig. 4I). In the γ-secretase-inhibited retinas, calretinin-positive cells were present but not organized into discrete laminae (Fig. 4J).

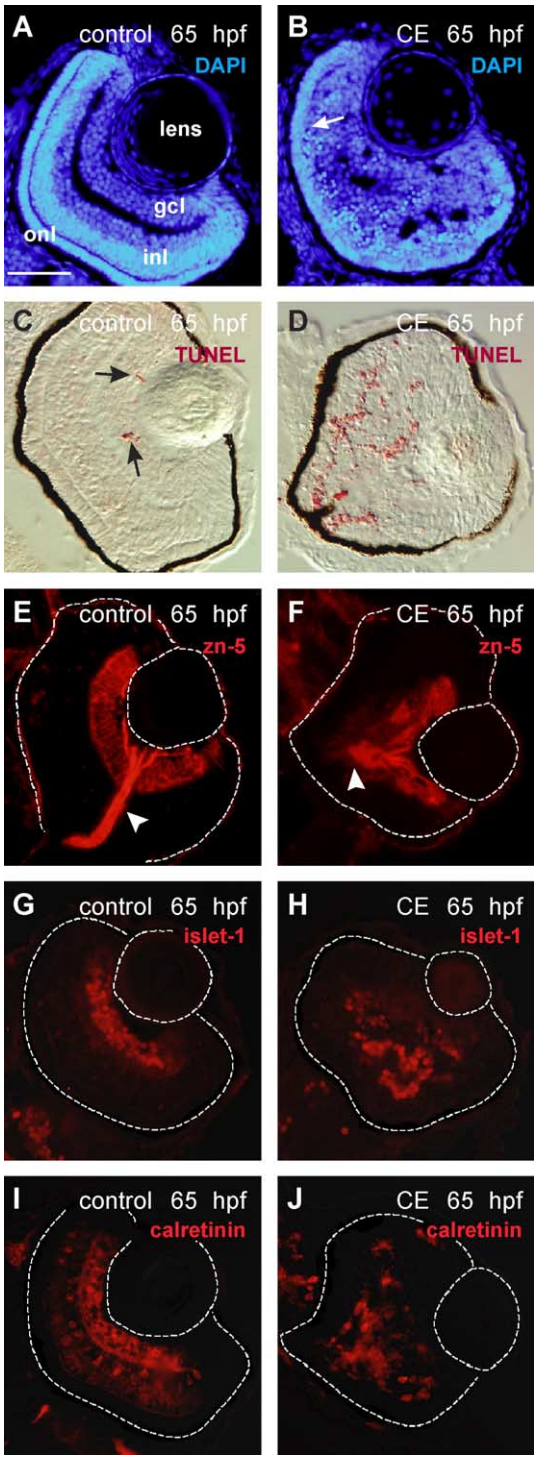

Fig. 4. Differentiation and laminar organization of the retina in control and γ-secretase-inhibited (CE) embryos at 65 hpf. (A, B) Retinal cell nuclei labeled by DAPI (blue). The retinal cell layers are distinguishable in the control retina (A) but in the CE-treated retina only the onl (arrow) can be identified (B). TUNEL-labeled control (C) and CE-treated (D) retinal cryosections (Fast Red—red). The arrows in (C) point to apoptotic cells in the wild-type retina. Ganglion cells and their axons in the optic nerve (arrowhead) were labeled by zn-5/neurolin in control (E) and CE-treated (F) retinas (N = 12 embryos). Ganglion cell nuclei were labeled by islet-1 antibody in control (G) and CE-treated (H) retinas (N = 10 embryos). The retinal boundary is outlined. The calretinin antibody labeled ganglion, amacrine, and bipolar cells (based on location and morphology) in the retinas of control embryos (I) and neurons in the CE-treated embryos (J) (N = 8 embryos). Scale bar = 50 μm (A–J). Abbreviations as in Fig. 1.

Photoreceptor differentiation in γ-secretase-inhibited embryos is initiated properly, but fails to progress and planar patterning is disrupted

We next examined control and γ-secretase-inhibited embryo retinal cryosections for the presence of photoreceptors using the double cone marker, zpr-1 (Figs. 5A, B). Although the cones in γ-secretase-inhibited retinas were properly positioned in a single row in the ONL at the apical surface, their morphology and spacing within that layer were abnormal (Fig. 5B), as described further below. Additionally, zs-4, which stains the apical surface of the retina (i.e., the outer limiting membrane), had a normal distribution, which showed that the epithelial polarity of the retina was not disrupted (Figs. 5C, D), consistent with the presence of a relatively intact ONL and the normal localization of differentiating photoreceptors at the apical surface of the retina (Fig. 5B).

The extent of retina covered by differentiated photoreceptors in γ-secretase-inhibited embryos was assessed using the same photoreceptor differentiation index described above for the *mib*$^{-/-}$ embryos. The differentiation of (rod opsin-expressing) rod photoreceptors at 65 hpf was not significantly affected by γ-secretase inhibitors as compared to control retinas (Fig. 2A; Table 2). In this respect, the γ-secretase-inhibited embryos differ from the *mib* mutants, in which progression of rod differentiation was blocked (Fig. 2A; Table 2). Although the timing of differentiation of rod photoreceptors was not disrupted by γ-secretase inhibition, their planar pattern was altered, in that clumps of rods were observed in CE-treated

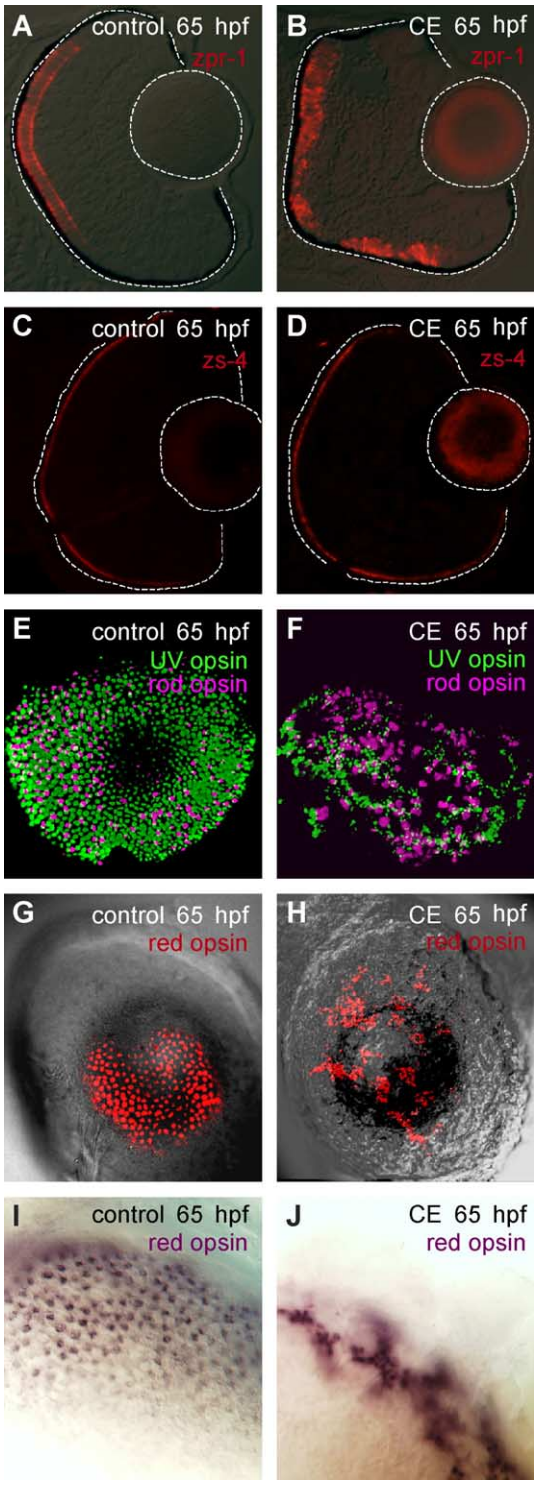

Fig. 5. Photoreceptor differentiation and planar organization in control and γ-secretase-inhibited (CE) embryos. (A, B) Double-cones labeled by zpr-1 at 65 hpf (N = 15 embryos). (C, D) The outer limiting membrane (apical surface) was labeled by zs-4 (N = 15 embryos). (E–J) Whole-mount preparations of control and CE-treated eyes processed for in situ hybridization using opsin-specific riboprobes. Rod (Fast Red-pseudo-colored magenta) and UV (FITC-green) opsin in control (E) and CE-treated (F) retinas at 65 hpf. Red opsin (Fast Red—red) in control (G) and CE-treated (H) retinas at 65 hpf. Higher magnification of control (I) and CE-treated (J) retinas stained for red opsin expression (NBT/BCIP—purple). Scale bar = 50 μm (A–H); 20 μm (I, J).

retinas (Fig. 5F), whereas in control retinas, they were more evenly distributed (Fig. 5E).

Differentiation of cone photoreceptors at 65 hpf in γ-secretase-inhibited embryos was even more disrupted than the rod photoreceptors. Although opsin expression was initiated normally, progression of the wave of differentiation of red and UV cones was significantly slowed in γ-secretase-inhibited retinas compared to control retinas, although not as severely as in the *mib*$^{-/-}$ embryos (Figs. 2B, C; Table 2). The planar spacing of the red and UV cones was also abnormal in the γ-secretase-inhibited embryos, with photoreceptors of the same spectral subtype often clumped together (Figs. 5F, H), a distribution that is never seen in control retinas (Figs. 5E, G). The highly abnormal distribution of red cones in a γ-secretase-inhibited embryo is shown at higher magnification in Fig. 5J, and is compared with the normal pattern in a control embryo in Fig. 5I. Similar alterations were seen in the distributions of blue and green cones (data not shown).

Müller glia do not differentiate in γ-secretase-inhibited embryos

We looked next for markers of differentiated Müller glia in γ-secretase-inhibited embryos. In wild-type zebrafish embryos, expression of the glial-specific marker zrf-1/GFAP, began as early as 48 hpf (see Supplementary Fig. 1B); the retinal staining pattern at 65 and 96 hpf is illustrated in Figs. 6A and C, respectively. The characteristic radial fibers of the Müller glia, which span the retinal epithelium from inner to outer surface, are clearly visible with zrf-1/GFAP, and the antibody also labels radial glia and astrocytes in the brain at 65 and 96 hpf (Figs. 6A, C). In contrast, in embryos treated with γ-secretase inhibitor from 9 to 65 hpf, or 9 to 96 hpf, zrf-1/GFAP staining was absent from the retina (Figs. 6B, D), whereas zrf-1/GFAP-positive glia were present, but disorganized and reduced in number, in the brain (Fig. 6B). Another early Müller glia-specific marker, glutamine synthetase, which appears at 60 hpf in the embryonic zebrafish retina (Peterson et al., 2001), was also absent from the retinas of γ-secretase-inhibited embryos (data not shown).

When embryos were removed from the γ-secretase inhibitor at 48 hpf and allowed to continue developing in embryo media until 96 hpf, retinal gliogenesis recovered and zrf-1/GFAP-positive Müller glia were generated by proliferating retinal progenitor cells in the germinal zone at the growing peripheral margin (Fig. 6F). Laminar organization was also improved at the periphery in the newly added retinal areas that contained Müller glia (Fig. 6I). However, in embryos that remained in the γ-secretase inhibitor from 9 to 65 hpf and were then transferred to embryo media to develop until 96 hpf, no recovery of lamination was observed and zrf-1/GFAP labeling was absent from the retina (Fig. 6H, J). To determine whether these embryos had the potential to generate Müller glia if

given a longer time to recover, some embryos were treated with the γ-secretase inhibitor from 9 to 65 hpf and then transferred to embryo media to develop until 120 hpf. These embryos had small eyes and some had extensive necrosis of the brain. Lamination was still absent in the retinas and staining with zrf-1/GFAP revealed small clusters of astrocytes surrounding the optic disc, but no zrf-1/GFAP-labeled Müller glia in the inner retina or at the periphery (see Supplementary Figs. 1C, D).

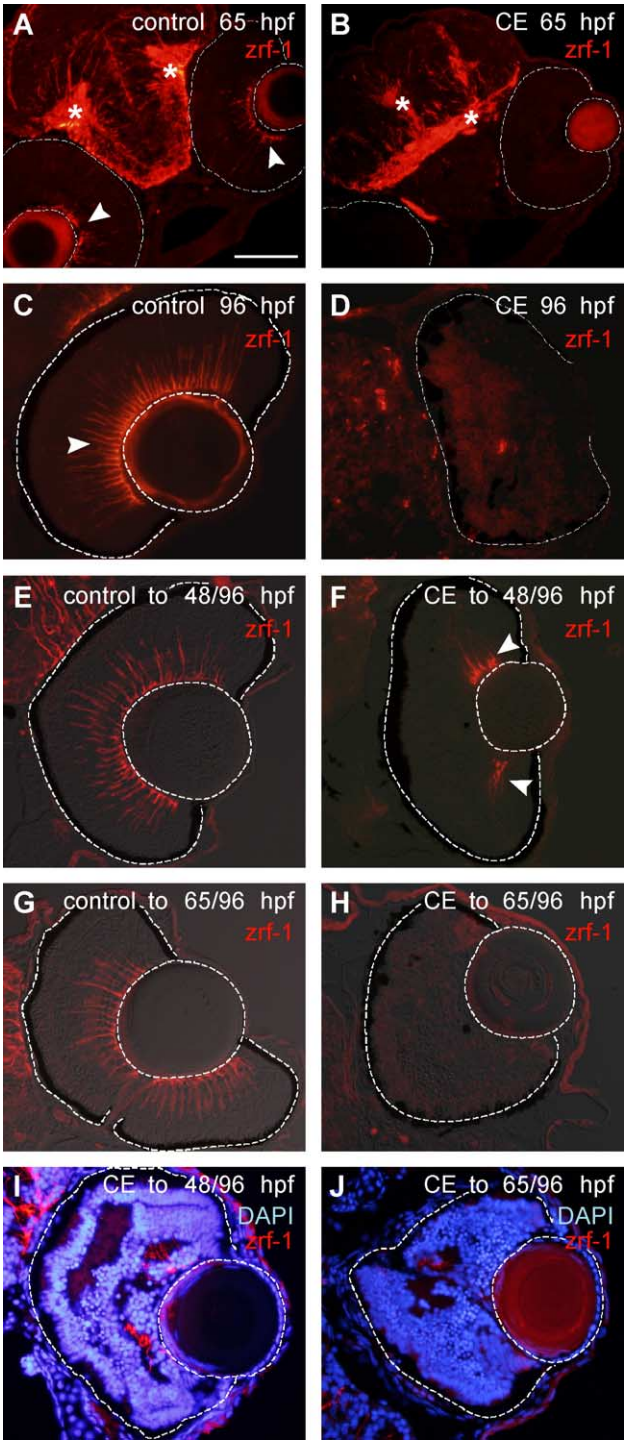

Similar to the *mib*$^{-/-}$ embryos, γ-secretase-inhibited embryos at 65 hpf expressed the Notch target gene *her6/hes1* in the ventricular zones of the brain but not in the retina (Figs. 7B, B′). In embryos treated with the γ-secretase inhibitor from 9 to 48 hpf and then transferred to embryo media and examined at 96 hpf, *her6/hes1* expression was present in the germinal zone at the ciliary margin of the retina and in areas of the INL where Müller glia were detected by zrf-1/GFAP immunoreactivity (Figs. 7D, D′). In controls at 96 hpf, *her6/hes1* was expressed in probable Müller glia and in the germinal zone (Figs. 7C, C′). In contrast, embryos that remained in the γ-secretase inhibitor to 65 hpf and were then transferred to embryo media and examined at 96 hpf, *her6/hes1* expression was present in the germinal zone, but not in the inner retina, which also showed no expression of zrf-1/GFAP (Figs. 7E, E′).

Inactivation of γ-secretase activity does not deplete the pool of retinal progenitors

Notch activation in the developing retina has been associated with maintenance of progenitor cells in an undifferentiated state, so one explanation for the failure of gliogenesis to recover in embryos treated with γ-secretase inhibitors up to 65 hpf might be that mitotic retinal progenitor pool has been depleted. To assess the status of the progenitor pool, we examined γ-secretase-inhibited retinas with an antibody to the mitotic marker, phosphorylated histone H3. Immunostaining revealed that the number of mitotic cells at 48 hpf was similar in control (N = 7; mean = 20 labeled nuclei per section; SD ± 2.64) and drug-treated embryos (N = 7; mean = 15.2 labeled nuclei per section; SD ± 4.76; $P > 0.05$) and both displayed numerous

Fig. 6. Müller glia fail to differentiate in the absence of Notch–Delta signaling. Immunostaining with zrf-1/GFAP (Cy3—red). In a control embryo at 65 hpf (A), radial glia in the brain are marked with an asterisk (*) and in the retina, endfeet of Müller glia at the vitreal surface are indicated by arrowheads. The apparent immunoreactivity in the lens is non-specific background. In an embryo treated in γ-secretase inhibitor (CE) up to 65 hpf (B), there is no staining with zrf-1/GFAP in the retina (outlined), but zrf-1/GFAP is present in the brain (*) (N = 20 embryos). At 96 hpf in a control retina (C) zrf-1/GFAP-labeled profiles (arrowhead) span the retina, whereas in a CE-treated embryo (D), there is no staining in the retina (outlined) (N = 20 embryos). (E, F) Retinas from embryos treated in control or drug solutions up to 48 hpf and then transferred to drug-free embryo media to continue development up to 96 hpf. In a CE-treated embryo (F) (N = 20 embryos examined), a few Müller glia (arrowheads) are indicated at the periphery of the retina (outlined) in contrast to the numerous Müller glia present in the control retina (E). (G, H) Retinas from embryos treated in control or drug solutions up to 65 hpf and then transferred to drug-free embryo media to continue development up to 96 hpf. In a drug-treated embryo (H), no zrf-1/GFAP staining is present in the retina (outlined) (N = 20 embryos). (I, J) Overlays of DAPI-stained and zrf-1/GFAP images show the relationship of Müller glia to the laminated regions of the retina in embryos treated with CE up to 48 hpf and then allowed to develop in drug-free embryo media up to 96 hpf (I) and embryos treated with CE up to 65 hpf and then allowed to develop in drug-free embryo media up to 96 hpf (J). Scale bar = 100 μm (A, B); 50 μm (C–J).

mitotic cells in the ONL (Figs. 8A, B). As development continued, the number of mitotic cells decreased in both control (N = 7; mean = 6 labeled nuclei per section; SD ± 2.87) and γ-secretase-inhibited embryos (N = 7; mean = 5 labeled nuclei per section; SD ± 2.0; $P > 0.05$) at 65 hpf (Figs. 8C, D). By 96 hpf, most of the mitotically active cells in both control and γ-secretase-inhibited embryos were located at the periphery of the retina (data not shown), where retinogenesis continues in the germinal zone at the ciliary margin (Marcus et al., 1999). These results indicate that the pool of mitotically active retinal progenitors is not depleted by inactivation of Notch–Delta signaling with γ-secretase inhibitors.

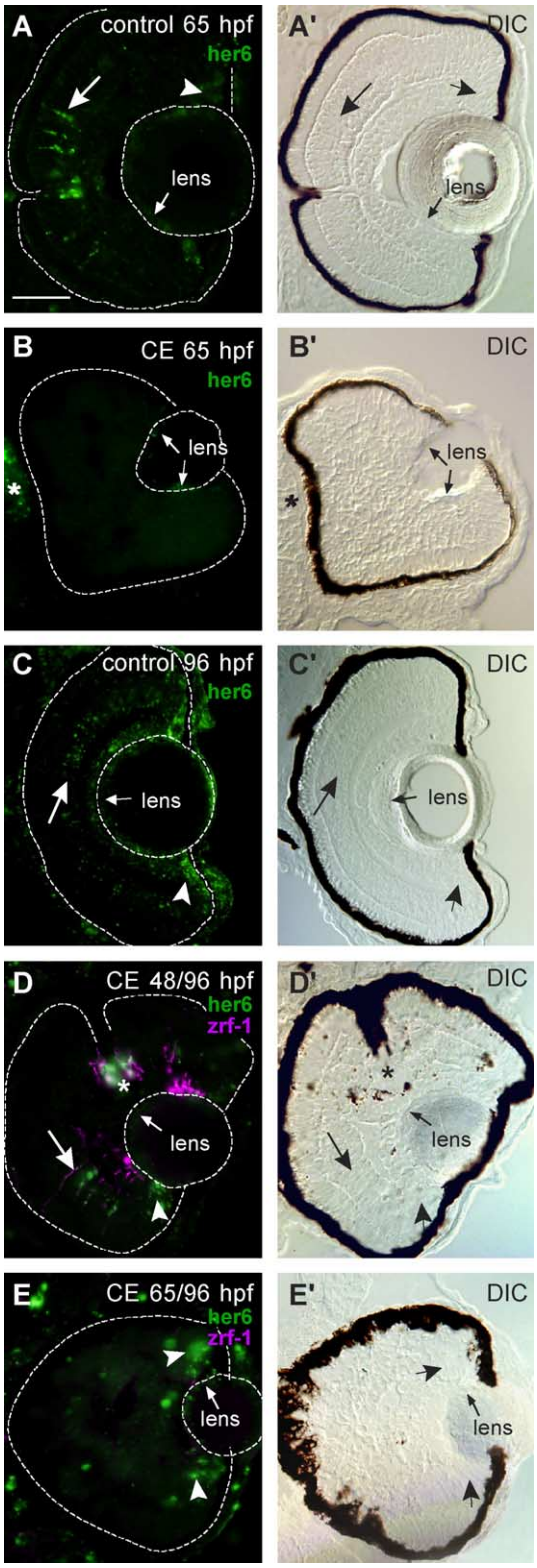

Discussion

The evolutionarily conserved Notch signaling pathway is involved in cell fate decisions in many different developing tissues in vertebrates and invertebrates (Baron, 2003). Notch proteins are Type I transmembrane receptors that bind Delta/Serrate/Lag-2 (DSL) transmembrane ligands on neighboring cells. Receptor-ligand binding triggers a series of proteolytic cleavages and results in the production of both Notch and Delta intracellular domains (NICD and DICD, respectively), which translocate to the nucleus of their respective cells to regulate gene transcription (Bland et al., 2003; De Strooper et al., 1999; Ebinu and Yankner, 2002; Ikeuchi and Sisodia, 2003; Kimberly and Wolfe, 2003; LaVoie and Selkoe, 2003; Steiner et al., 1999).

The classic view of Notch–Delta signaling in the developing nervous system is that activation of Notch blocks neuronal differentiation through a mechanism of lateral inhibition, in which cells that begin to differentiate as neurons express high levels of the ligand Delta, triggering Notch signaling in adjacent cells and activating transcription of the *Hes* genes, which transcriptionally repress other (proneural) bHLH transcription factors required for neuronal

Fig. 7. Lack of *her6/hes1* expression reflects inhibition of Notch signaling. Cryosections of control and γ-secretase-inhibited (CE) embryos labeled for *her6/hes1* expression (FITC—green) by *in situ* hybridization. DIC images indicate the location of *her6/hes1* expression in the retina (outlined) in the paired panels to the left. (A, A′) At 65 hpf, *her6/hes1* expression in the inl (large arrow) and germinal zone (arrowhead) of the retina and in the lens epithelium (small arrow) in control embryos. (B, B′) *her6/hes1* expression in the lens epithelium (small arrows) and brain (*) of CE-treated embryos (N = 15 embryos). (C, C′) At 96 hpf, *her6/hes1* is expressed in the inl, often in radial streaks (large arrow), and in the germinal zone (arrowhead) of the retina and in the lens epithelium (small arrow) of control embryos (N = 15 embryos). A faint reaction product is also seen in the gcl, but this may be localized to the endfeet of Müller glia—a similar pattern of *gfap* mRNA expression is observed in retinas at this stage (R.L.B., unpublished observations). (D, D′) In embryos treated with CE up to 48 hpf and then allowed to develop in drug-free embryo media up to 96 hpf, *her6/hes1* is expressed in the inl (large arrow), germinal zone of the retina (arrowhead), the optic nerve head (*; astrocytes) and in the lens epithelium (small arrow). Co-labeling with zrf-1/GFAP (Cy-3-pseudo-colored magenta) reveals a correlation between the location of zrf-1/GFAP and *her6/hes1* expression in the inl (N = 15 embryos). (E, E′) In embryos treated with CE up to 65 hpf and then allowed to develop in drug-free embryo media up to 96 hpf, *her6/hes1* is expressed only in the retinal germinal zone (arrowhead) and lens epithelium (small arrows) and no zrf-1/GFAP immunoreactivity is detected in the retina (N = 15 embryos). Scale bar = 50 μm (A–E).

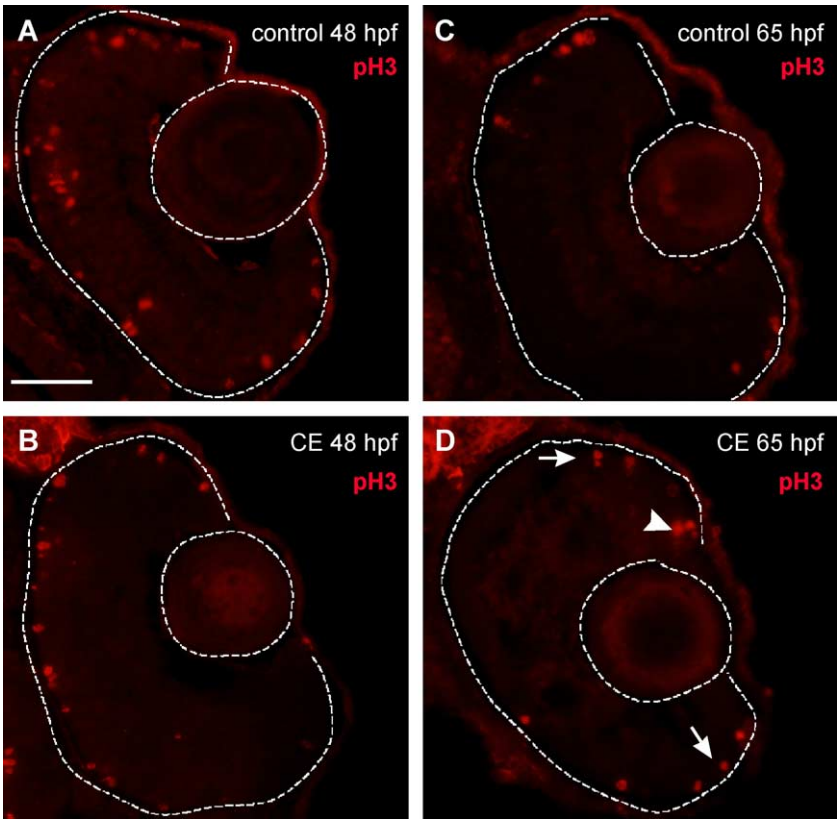

Fig. 8. Mitotic activity in the retinas of control and γ-secretase-inhibited (CE) embryos. (A–D) Retinal cryosections labeled with phosphorylated histone H3 (pH3) antibody (Cy3—red). (A) Control and (B) CE-treated retinas labeled with anti-pH3 at 48 hpf. Mitotic cells were present in the outer retina in control and drug-treated retinas. By 65 hpf, mitotic activity was restricted to the germinal zone at the ciliary margin (arrow) and outer nuclear layer (arrowheads) in control (C) and CE-treated (D). Scale bar = 50 μm (A–D).

differentiation (Lewis, 1996). More recently, Notch signaling has been shown to operate in some situations by an instructive mechanism, actively promoting glial differentiation in the responding cell (Furukawa et al., 2000; Gaiano and Fishell, 2002; Gaiano et al., 2000; Kageyama et al., 1997; Morrison et al., 2000; Scheer et al., 2001). There is a growing awareness that intricate and poorly understood regulatory influences are at least partially responsible for the complexity of cellular responses to activation of these pathways (Baron, 2003; Justice and Jan, 2002).

In the developing retina, Notch signaling has been shown to maintain the pool of proliferating progenitors and prevent differentiation of retinal neurons or to promote differentiation of Müller glia, whereas Delta signaling promotes neuronal differentiation (Ahmad et al., 2004; Livesey and Cepko, 2001; Mu and Klein, 2004; Perron and Harris, 2000; Pujic and Malicki, 2004). Many of these studies have utilized transfection techniques to alter gene expression in individual or small groups of retinal progenitor cells. In these cases, Notch or Delta signaling is disrupted in a subset of cells that are bordered by cells with normal function, thus complicating the interpretation of the results. For example, in *Xenopus* embryos injected with *X-Delta-1* mRNA, the outcome depended on whether a misexpressing cell was in the center of a clone isolated from surrounding normal cells, or near the borders of the clone in direct contact with normal cells: progenitors in the center of the clone did not differentiate whereas those at the borders differentiated into neurons (Dorsky et al., 1997). Thus, the response a cell makes when the function of one component of the Notch–Delta signaling cascade is altered depends on its context within the neighboring pool of cells and the state of activation of Notch and Delta signaling cascades in those cells, variables that are not controlled in this type of experiment.

We reasoned that by broadly inhibiting the activation of both Notch and Delta, thereby blocking both arms of the bidirectional signaling pathway in all cells, we would uncover essential roles of Notch–Delta signals in retinal development. We used two independent methods, one genetic and the other pharmacologic, and the results of both were the same. To our knowledge, previous studies of the role of Notch–Delta signaling in retinal development have not used these methods. The lack of expression of the Notch target gene *her6/hes1* in the retina in both preparations suggests that Notch signaling was largely or completely inactivated in our experiments. Because so little is currently known about the downstream targets of Delta activation, we were unable to directly test whether Delta-mediated signaling was also blocked, although the existing

data on the activity of the *mind bomb* ubiquitin ligase and the targets of γ-secretase processing suggest that Delta signaling was also disrupted (Itoh et al., 2003; LaVoie and Selkoe, 2003).

Our principal finding was that retinal neurons differentiated when Notch–Delta signaling was disrupted, but Müller glia did not. While we cannot exclude the possibility that Müller glia are produced but fail to differentiate, we found no evidence of expression of early markers of Müller glia, such as glutamine synthetase, GFAP or *her6/hes1*, suggesting that retinal gliogenesis was blocked. In contrast, in both *mib*$^{-/-}$ and γ-secretase-inhibited embryos, markers of neuronal differentiation were expressed in the retina at the appropriate developmental stages, although normal laminar organization of the inner retina was disrupted. Most retinal ganglion cells were positioned near the inner retinal surface, but they were not organized into a continuous, discrete layer. The inner nuclear layer was similarly disrupted. In contrast, stratification of the outer nuclear layer was approximately normal, and a single row of differentiating photoreceptors with columnar nuclei formed along the apical retinal surface. However, the photoreceptors were not appropriately positioned in the planar dimension. In the normal zebrafish retina, photoreceptors are arranged in a highly organized, planar mosaic pattern with precise spatial relationships among the four different cone photoreceptors (red, green, blue, and ultraviolet) and the rod photoreceptors (Branchek and Bremiller, 1984; Fadool, 2003; Pujic and Malicki, 2004; Raymond et al., 1995). This regular arrangement and the progression of photoreceptor differentiation, which normally proceeds in a wave across the retina, were disrupted in *mib*$^{-/-}$ mutants and γ-secretase-treated embryos. Although the cellular and molecular mechanisms that pattern the photoreceptor mosaic in the teleost retina are unknown, Notch–Delta signaling is important for photoreceptor cell identity and spacing in the compound eye of *Drosophila* (Baker and Zitron, 1995; Basler and Hafen, 1991; Brennan and Moses, 2000), and our results suggest that it may play a similar role in planar patterning of photoreceptors in zebrafish.

When embryos treated with γ-secretase inhibitor were removed from the drug by 48 hpf, prior to the completion of embryonic development and onset of visual function, retinal histogenesis recovered. We noted that the lamination defect and the block of gliogenesis were correlated, and once released from inhibition of Notch–Delta activation, retinal progenitors in the germinal zone at the ciliary margin generated both differentiated Müller glia and a normally laminated retina. Although we have no direct evidence for causality, our data are consistent with a role for Müller glia in organizing the stratification of the inner retina. This inference is potentially in conflict with ^{3}H-thymidine birthdating studies in rodents, which suggest that Müller glia are among the last retinal cells to be produced and would therefore not be present to organize the differentiating retinal neurons (Sidman, 1961; Young, 1985). However, anatomical evidence suggests that cells with some properties of Müller glia are present at early stages in retinal development (Willbold and Layer, 1998). The anatomical studies suggest that Müller glia undergo a gradual maturation from neuroepithelial cells (perhaps with some properties of radial glia) to mature Müller glia, and thus are present in an immature form at the onset of retinal differentiation (Peterson et al., 2001; Willbold and Layer, 1998). The presence in the early developing retina of cells with the properties of Müller glia has been supported by several studies using techniques such as scanning electron microscopy analysis (Meller and Tetzlaff, 1976; Uga and Smelser, 1973) and morphological analysis by Golgi-staining (Prada et al., 1989). The discrepancy between the ^{3}H-thymidine birthdating studies and the histological data may be explained by the continuing capacity of differentiating Müller glia to proliferate in the developing retina. The birthdating studies measure only the terminal mitotic division of a cell, which is a useful concept for neurons but less applicable to mitotically competent glia cells. Our data show that defects in retinal lamination resulting from inactivation of Notch–Delta signaling are correlated with an absence of Müller glia and are in agreement with in vitro work using cultures of reaggregated retinal progenitor cells from embryonic chick retinas, which showed that Müller glial cells provide a scaffolding that is required for proper retinal lamination (Layer et al., 1990, 2002; Willbold et al., 2000). Similarly, in the retinas of *Hes1*-null mutant mice in which the number of Müller glia is significantly reduced, retinal lamination is also disrupted (Takatsuka et al., 2004).

The absence of expression of the Notch target gene, *her6/hes1*, in the retinas of γ-secretase-inhibited embryos provides evidence that this pharmacological intervention was effective at inactivating Notch signaling. However, other Type I transmembrane proteins are also processed by γ-secretase/presenilin and so we cannot exclude the possibility that some of the effects we observed on retinal development in the γ-secretase-inhibited embryos may not solely be due to disruption of the Notch–Delta signaling pathway. For example, the amyloid precursor protein (APP) has been implicated in axonogenesis, dendritic arborization, and synaptic differentiation in the developing nervous system (De Strooper and Annaert, 2000; Fortini, 2002; Mattson, 2001). Cadherins are also processed by γ-secretase/presenilin, and inhibition of γ-secretase activity may have resulted in altered cell–cell adhesion that could have disrupted the organization of the retina. Mutations in the zebrafish *N-cadherin* gene (*glass onion*, *glo*, and *parachute*, *pac* alleles) severely affect both retinal lamination and polarity (Erdmann et al., 2003; Malicki et al., 2003), and injection of function-blocking N-cadherin antibody into developing chick retinas also disrupts apical polarity, interferes with laminar formation and produces multiple rosettes—spherical clusters of photoreceptors and Müller glia organized around a vesicular lumen (Matsunaga et al., 1988). Since these defects are more severe than the

phenotypes we observed with inhibition of γ-secretase activity, our observations are not likely to be explained by a defect in cadherin function.

Our experiments targeted two independent, cellular mechanisms, γ-secretase/presenilin proteolysis and E3 ubiquitin ligase activity, and the retinal phenotypes produced by each experimental model were nearly identical. This suggests that a common pathway was disrupted in both experimental models. We suggest that the Notch–Delta signaling pathway is the target of γ-secretase inhibition and of the *mib* mutation in the retina and is responsible for the observed defects. The strongest evidence supporting this conclusion is that the expression of the Notch target gene *her6/hes1* was selectively and completely abolished in γ-secretase-inhibited and $mib^{-/-}$ retinas. Expression of *Hes* genes has been shown to depend on the association of NICD with transcriptional machinery in the cell nucleus, and in the absence of NICD *Hes1* is not expressed (Iso et al., 2003; Kageyama and Ohtsuka, 1999; Takke et al., 1999) More difficult to explain is our finding that although *her6/hes1* expression was absent in the retina, it was present in the brains and lenses of both γ-secretase-inhibited and $mib^{-/-}$ embryos. One possible explanation is that some tissues are less sensitive to manipulations of Notch–Delta signaling because of redundant signaling pathways or expression of multiple Notch–Delta genes, whereas the retina may have fewer compensatory mechanisms and/or express only a subset of the Notch–Delta genes found in the brain. For example, in a recent study, the distribution of Presenilin-1 and -2 was compared to the distribution of the several members of the Notch family (Notch-1 to Notch-4) in the human embryonic/foetal central nervous system by immunohistochemistry (Kostyszyn et al., 2004). The data from this study demonstrate that only Notch-1 is co-expressed with Presenilin-1 and -2 in the human fetus during the first trimester. It is possible that a similar relationship between selected Notch family members and presenilins exits in the zebrafish retina, which makes this tissue more sensitive to the effects of blocking γ-secretase activity. Further characterization of the expression patterns of the known *notch*, *delta*, and *presenilin* genes during zebrafish development would help to answer this question.

In summary, the results reported here show that Notch–Delta signaling is necessary for differentiation of Müller glia but not retinal neurons, and our results suggest that Müller glia may be necessary for proper stratification and organization of the inner retina in developing zebrafish.

Acknowledgments

Supported by EY04318 and P60DK20572 to P.A.R., NIH 5T32DC005341 and 5T32EY013934 to R.L.B, and NS41355 to M.S.W. We thank Linda Barthel, Dilip Pawar and Chen Kuang for technical assistance, John Kuwada, David Hyde, Thomas Vihtelic, Paul Linser and José Campos-Ortega for reagents, and Peter Hitchcock for comments on the manuscript.

Appendix A. Supplementary data

Supplementary data associated with this article can be found, in the online version, at doi:10.1016/j.ydbio.2004.11.018.

References

Ahmad, I., Das, A.V., James, J., Bhattacharya, S., Zhao, X., 2004. Neural stem cells in the mammalian eye: types and regulation. Semin. Cell Dev. Biol. 15, 53–62.

Andressen, C., Blumcke, I., Celio, M.R., 1993. Calcium-binding proteins: selective markers of nerve cells. Cell Tissue Res. 271, 181–208.

Austin, C.P., Feldman, D.E., Ida Jr., J.A., Cepko, C.L., 1995. Vertebrate retinal ganglion cells are selected from competent progenitors by the action of Notch. Development 121, 3637–3650.

Baker, N.E., Zitron, A.E., 1995. *Drosophila* eye development: Notch and Delta amplify a neurogenic pattern conferred on the morphogenetic furrow by scabrous. Mech. Dev. 49, 173–189.

Bao, Z.Z., Cepko, C.L., 1997. The expression and function of Notch pathway genes in the developing rat eye. J. Neurosci. 17, 1425–1434.

Baron, M., 2003. An overview of the Notch signalling pathway. Semin. Cell Dev. Biol. 14, 113–119.

Barthel, L.K., Raymond, P.A., 1990. Improved method for obtaining 3-microns cryosections for immunocytochemistry. J. Histochem. Cytochem. 38, 1383–1388.

Barthel, L.K., Raymond, P.A., 1993. Subcellular localization of alpha-tubulin and opsin mRNA in the goldfish retina using digoxigenin-labeled cRNA probes detected by alkaline phosphatase and HRP histochemistry. J. Neurosci. Methods 50, 145–152.

Barthel, L.K., Raymond, P.A., 2000. In situ hybridization studies of retinal neurons. Methods Enzymol. 316, 579–590.

Basler, K., Hafen, E., 1991. Specification of cell fate in the developing eye of *Drosophila*. BioEssays 13, 621–631.

Bland, C.E., Kimberly, P., Rand, M.D., 2003. Notch-induced proteolysis and nuclear localization of the Delta ligand. J. Biol. Chem. 278, 13607–13610.

Branchek, T., Bremiller, R., 1984. The development of photoreceptors in the zebrafish, *Brachydanio rerio*. I. Structure. J. Comp. Neurol. 224, 107–115.

Brennan, C.A., Moses, K., 2000. Determination of *Drosophila* photoreceptors: timing is everything. Cell. Mol. Life Sci. 57, 195–214.

Burrill, J.D., Easter Jr., S.S., 1994. Development of the retinofugal projections in the embryonic and larval zebrafish (*Brachydanio rerio*). J. Comp. Neurol. 346, 583–600.

De Strooper, B., Annaert, W., 2000. Proteolytic processing and cell biological functions of the amyloid precursor protein. J. Cell Sci. 113 (Pt. 11), 1857–1870.

De Strooper, B., Annaert, W., Cupers, P., Saftig, P., Craessaerts, K., Mumm, J.S., Schroeter, E.H., Schrijvers, V., Wolfe, M.S., Ray, W.J., Goate, A., Kopan, R., 1999. A presenilin-1-dependent gamma-secretes-like protease mediates release of Notch intracellular domain. Nature 398, 518–522.

Dorsky, R.I., Chang, W.S., Rapaport, D.H., Harris, W.A., 1997. Regulation of neuronal diversity in the *Xenopus* retina by Delta signalling. Nature 385, 67–70.

Ebinu, J.O., Yankner, B.A., 2002. A RIP tide in neuronal signal transduction. Neuron 34, 499–502.

Erdmann, B., Kirsch, F.P., Rathjen, F.G., More, M.I., 2003. N-cadherin is essential for retinal lamination in the zebrafish. Dev. Dyn. 226, 570–577.

Fadool, J.M., 2003. Development of a rod photoreceptor mosaic revealed in transgenic zebrafish. Dev. Biol. 258, 277–290.

Fashena, D., Westerfield, M., 1999. Secondary motoneuron axons localize DM-GRASP on their fasciculated segments. J. Comp. Neurol. 406, 415–424.

Fortini, M.E., 2002. Gamma-secretase-mediated proteolysis in cell-surface-receptor signalling. Nat. Rev., Mol. Cell Biol. 3, 673–684.

Furukawa, T., Mukherjee, S., Bao, Z.Z., Morrow, E.M., Cepko, C.L., 2000. *rax*, *Hes1*, and *notch1* promote the formation of Muller glia by postnatal retinal progenitor cells. Neuron 26, 383–394.

Gaiano, N., Fishell, G., 2002. The role of notch in promoting glial and neural stem cell fates. Annu. Rev. Neurosci. 25, 471–490.

Gaiano, N., Nye, J.S., Fishell, G., 2000. Radial glial identity is promoted by Notch1 signaling in the murine forebrain. Neuron 26, 395–404.

Geling, A., Steiner, H., Willem, M., Bally-Cuif, L., Haass, C., 2002. A gamma-secretase inhibitor blocks Notch signaling in vivo and causes a severe neurogenic phenotype in zebrafish. EMBO Rep. 3, 688–694.

Haddon, C., Jiang, Y.J., Smithers, L., Lewis, J., 1998. Delta–Notch signalling and the patterning of sensory cell differentiation in the zebrafish ear: evidence from the mind bomb mutant. Development 125, 4637–4644.

Hatakeyama, J., Kageyama, R., 2004. Retinal cell fate determination and bHLH factors. Semin. Cell Dev. Biol. 15, 83–89.

Hojo, M., Ohtsuka, T., Hashimoto, N., Gradwohl, G., Guillemot, F., Kageyama, R., 2000. Glial cell fate specification modulated by the bHLH gene Hes5 in mouse retina. Development 127, 2515–2522.

Hu, M., Easter, S.S., 1999. Retinal neurogenesis: the formation of the initial central patch of postmitotic cells. Dev. Biol. 207, 309–321.

Ikeuchi, T., Sisodia, S.S., 2003. The Notch ligands, Delta1 and Jagged2, are substrates for presenilin-dependent "gamma-secretase" cleavage. J. Biol. Chem. 278, 7751–7754.

Iso, T., Kedes, L., Hamamori, Y., 2003. *HES* and *HERP* families: multiple effectors of the Notch signaling pathway. J. Cell. Physiol. 194, 237–255.

Itoh, M., Kim, C.H., Palardy, G., Oda, T., Jiang, Y.J., Maust, D., Yeo, S.Y., Lorick, K., Wright, G.J., Ariza-McNaughton, L., Weissman, A.M., Lewis, J., Chandrasekharappa, S.C., Chitnis, A.B., 2003. Mind bomb is a ubiquitin ligase that is essential for efficient activation of Notch signaling by Delta. Dev. Cell 4, 67–82.

Jiang, Y.J., Brand, M., Heisenberg, C.P., Beuchle, D., Furutani-Seiki, M., Kelsh, R.N., Warga, R.M., Granato, M., Haffter, P., Hammerschmidt, M., Kane, D.A., Mullins, M.C., Odenthal, J., van Eeden, F.J., Nusslein-Volhard, C., 1996. Mutations affecting neurogenesis and brain morphology in the zebrafish, *Danio rerio*. Development 123, 205–216.

Justice, N.J., Jan, Y.N., 2002. Variations on the Notch pathway in neural development. Curr. Opin. Neurobiol. 12, 64–70.

Kageyama, R., Ohtsuka, T., 1999. The Notch–Hes pathway in mammalian neural development. Cell Res. 9, 179–188.

Kageyama, R., Ishibashi, M., Takebayashi, K., Tomita, K., 1997. bHLH transcription factors and mammalian neuronal differentiation. Int. J. Biochem. Cell Biol. 29, 1389–1399.

Kimberly, W.T., Wolfe, M.S., 2003. Identity and function of gamma-secretase. J. Neurosci. Res. 74, 353–360.

Kostyszyn, B., Cowburn, R.F., Seiger, A., Kjaeldgaard, A., Sundstrom, E., 2004. Distribution of presenilin 1 and 2 and their relation to Notch receptors and ligands in human embryonic/foetal central nervous system. Brain Res., Dev. Brain Res. 151, 75–86.

LaVoie, M.J., Selkoe, D.J., 2003. The Notch ligands, Jagged and Delta, are sequentially processed by alpha-secretase and presenilin/gamma-secretase and release signaling fragments. J. Biol. Chem. 278, 34427–34437.

Layer, P.G., Alber, R., Mansky, P., Vollmer, G., Willbold, E., 1990. Regeneration of a chimeric retina from single cells in vitro: cell-lineage-dependent formation of radial cell columns by segregated chick and quail cells. Cell Tissue Res. 259, 187–198.

Layer, P.G., Robitzki, A., Rothermel, A., Willbold, E., 2002. Of layers and spheres: the reaggregate approach in tissue engineering. Trends Neurosci. 25, 131–134.

Lewis, J., 1996. Neurogenic genes and vertebrate neurogenesis. Curr. Opin. Neurobiol. 6, 3–10.

Livesey, F.J., Cepko, C.L., 2001. Vertebrate neural cell-fate determination: lessons from the retina. Nat. Rev., Neurosci. 2, 109–118.

Malicki, J., 1999. Development of the retina. Methods Cell Biol. 59, 273–299.

Malicki, J., Jo, H., Pujic, Z., 2003. Zebrafish N-cadherin, encoded by the glass onion locus, plays an essential role in retinal patterning. Dev. Biol. 259, 95–108.

Marcus, R.C., Easter Jr., S.S., 1995. Expression of glial fibrillary acidic protein and its relation to tract formation in embryonic zebrafish (*Danio rerio*). J. Comp. Neurol. 359, 365–381.

Marcus, R.C., Delaney, C.L., Easter Jr., S.S., 1999. Neurogenesis in the visual system of embryonic and adult zebrafish (*Danio rerio*). Vis. Neurosci. 16, 417–424.

Matsunaga, M., Hatta, K., Takeichi, M., 1988. Role of N-cadherin cell adhesion molecules in the histogenesis of neural retina. Neuron 1, 289–295.

Mattson, M.P., 2001. A multi-talented secreted protein. Trends Neurosci. 24, 441–442.

Meller, K., Tetzlaff, W., 1976. Scanning electron microscopic studies on the development of the chick retina. Cell Tissue Res. 170, 145–159.

Morrison, S.J., Perez, S.E., Qiao, Z., Verdi, J.M., Hicks, C., Weinmaster, G., Anderson, D.J., 2000. Transient Notch activation initiates an irreversible switch from neurogenesis to gliogenesis by neural crest stem cells. Cell 101, 499–510.

Mu, X., Klein, W.H., 2004. A gene regulatory hierarchy for retinal ganglion cell specification and differentiation. Semin. Cell Dev. Biol. 15, 115–123.

Nuesslein-Volhard, C., Dahm, R., 2002. Zebrafish: A Practical Approach. Oxford University Press, New York.

Perron, M., Harris, W.A., 2000. Determination of vertebrate retinal progenitor cell fate by the Notch pathway and basic helix–loop-helix transcription factors. Cell. Mol. Life Sci. 57, 215–223.

Peterson, R.E., Fadool, J.M., McClintock, J., Linser, P.J., 2001. Muller cell differentiation in the zebrafish neural retina: evidence of distinct early and late stages in cell maturation. J. Comp. Neurol. 429, 530–540.

Prada, F.A., Magalhaes, M.M., Coimbra, A., Genis-Galvez, J.M., 1989. Morphological differentiation of the Muller cell: Golgi and electron microscopy study in the chick retina. J. Morphol. 201, 11–22.

Pujic, Z., Malicki, J., 2004. Retinal pattern and the genetic basis of its formation in zebrafish. Semin. Cell Dev. Biol. 15, 105–114.

Rapaport, D.H., Dorsky, R.I., 1998. Inductive competence, its significance in retinal cell fate determination and a role for Delta–Notch signaling. Semin. Cell Dev. Biol. 9, 241–247.

Raymond, P.A., Barthel, L.K., Curran, G.A., 1995. Developmental patterning of rod and cone photoreceptors in embryonic zebrafish. J. Comp. Neurol. 359, 537–550.

Scheer, N., Groth, A., Hans, S., Campos-Ortega, J.A., 2001. An instructive function for Notch in promoting gliogenesis in the zebrafish retina. Development 128, 1099–1107.

Schier, A., Neuhauss, S., Harvey, M., Malicki, J., Solnica-Krezel, L., Stainier, D., Zwartkruis, F., Abdelilah, S., Stemple, D., Rangini, Z., Yang, H., Driever, W., 1996. Mutations affecting the development of the embryonic zebrafish brain. Development 123, 165–178.

Schmitt, E.A., Dowling, J.E., 1996. Comparison of topographical patterns of ganglion and photoreceptor cell differentiation in the retina of the zebrafish, *Danio rerio*. J. Comp. Neurol. 371, 222–234.

Schmitt, E.A., Dowling, J.E., 1999. Early retinal development in the zebrafish, *Danio rerio*: light and electron microscopic analyses. J. Comp. Neurol. 404, 515–536.

Schneider, M.L., Turner, D.L., Vetter, M.L., 2001. Notch signaling can inhibit *Xath5* function in the neural plate and developing retina. Mol. Cell. Neurosci. 18, 458–472.

Schwaller, B., Buchwald, P., Blumcke, I., Celio, M.R., Hunziker, W., 1993. Characterization of a polyclonal antiserum against the purified human recombinant calcium binding protein calretinin. Cell Calcium 14, 639–648.

Seiffert, D., Bradley, J.D., Rominger, C.M., Rominger, D.H., Yang, F., Meredith Jr., J.E., Wang, Q., Roach, A.H., Thompson, L.A., Spitz, S.M., Higaki, J.N., Prakash, S.R., Combs, A.P., Copeland, R.A., Arneric, S.P., Hartig, P.R., Robertson, D.W., Cordell, B., Stern, A.M., Olson, R.E., Zaczek, R., 2000. Presenilin-1 and -2 are molecular targets for gamma-secretase inhibitors. J. Biol. Chem. 275, 34086–34091.

Sidman, R.L., 1961. Histogenesis of mouse retina studied with thymidine-H3. In: Smelser, G.K. (Ed.), The Structure of the Eye. Academic Press, New York, pp. 487–505.

Silva, A.O., Ercole, C.E., McLoon, S.C., 2003. Regulation of ganglion cell production by Notch signaling during retinal development. J. Neurobiol. 54, 511–524.

Steiner, H., Duff, K., Capell, A., Romig, H., Grim, M.G., Lincoln, S., Hardy, J., Yu, X., Picciano, M., Fechteler, K., Citron, M., Kopan, R., Pesold, B., Keck, S., Baader, M., Tomita, T., Iwatsubo, T., Baumeister, R., Haass, C., 1999. A loss of function mutation of Presenilin-2 interferes with amyloid beta-peptide production and Notch signaling. J. Biol. Chem. 274, 28669–28673.

Stenkamp, D.L., Hisatomi, O., Barthel, L.K., Tokunaga, F., Raymond, P.A., 1996. Temporal expression of rod and cone opsins in embryonic goldfish retina predicts the spatial organization of the cone mosaic. Invest. Ophthalmol. Visual Sci. 37, 363–376.

Takatsuka, K., Hatakeyama, J., Bessho, Y., Kageyama, R., 2004. Roles of the bHLH gene Hes1 in retinal morphogenesis. Brain Res. 1004, 148–155.

Takke, C., Dornseifer, P., v Weizsacker, E., Campos-Ortega, J.A., 1999. *her4*, a zebrafish homologue of the *Drosophila* neurogenic gene *E(spl)*, is a target of NOTCH signalling. Development 126, 1811–1821.

Turner, D.L., Cepko, C.L., 1987. A common progenitor for neurons and glia persists in rat retina late in development. Nature 328, 131–136.

Uga, S., Smelser, G.K., 1973. Electron microscopic study of the development of retinal Mullerian cells. Invest. Ophthalmol. 12, 295–307.

Varga, Z.M., Wegner, J., Westerfield, M., 1999. Anterior movement of ventral diencephalic precursors separates the primordial eye field in the neural plate and requires cyclops. Development 126, 5533–5546.

Westerfield, M., 2000. The Zebrafish Book. A Guide for the Laboratory Use of Zebrafish (*Danio rerio*). Univ. of Oregon Press, Eugene.

Willbold, E., Layer, P.G., 1998. Muller glia cells and their possible roles during retina differentiation in vivo and in vitro. Histol. Histopathol. 13, 531–552.

Willbold, E., Rothermel, A., Tomlinson, S., Layer, P.G., 2000. Muller glia cells reorganize reaggregating chicken retinal cells into correctly laminated in vitro retinae. Glia 29, 45–57.

Woo, K., Fraser, S.E., 1995. Order and coherence in the fate map of the zebrafish nervous system. Development 121, 2595–2609.

Yazulla, S., Studholme, K.M., 2001. Neurochemical anatomy of the zebrafish retina as determined by immunocytochemistry. J. Neurocytol. 30, 551–592.

Young, R.W., 1985. Cell differentiation in the retina of the mouse. Anat. Rec. 212, 199–205.